JOURNAL OF KUFA–PHYSICS
www.uokufa.edu.iq/journals/index.php/jkp | ISSN: 2077–5830

Electron collision with Ammonia and phosphine at wide range of energies

***Ahlam K. Yassir** **Alaa A. Khalaf**

Department of Physics, College of Science, University of Basrh.

*Corresponding Author E-mail: addressahlam.ashour.sci@uobasrah.edu.iq

ARTICLE INF

Article history:
Received: 19 OCT, 2022
Revised: 30 NOV, 2022
Accepted: 11 DeC, 2021
Available Online: 5 FEB, 2023

Keywords:

Cross section
Electron
Molecule
Scattering
Optical model

ABSTRACT

Differential electron elastic scattering cross sections are attained by ammonia and phosphine molecules for 15 eV to 500 eV and 5 eV to 500 eV, respectively. The required calculations were done with the use of partial waveforms characterizing the target molecule and a single Hartree-Fock Molecular Function Center. Results from this model make evident the significance of the exchange, as well as the contributions of correlation and polarization, particularly at low scattering angles and incident energy, because the potentials utilized contain a constant part—numerically generated through quantum computing. Good agreement was discovered between the calculated differential cross sections and a wide database of experimental data. Different spherical scattering angles and power spectrums are analyzed in this paper.

DOI: http://dx.doi.org/10.31257/2018/JKP/2022/140208

تصادم الإلكترون مع الأمونيا والفوسفين على نطاق واسع من الطاقات

احلام خضير ياسر **علاء عبد الحسن خلف**

جامعة البصرة /كلية العلوم / قسم الفيزياء

الكلمات المفتاحية:

مقطع عرضي
الكترون
الجزيئة
الاستطارة
النموذج البصري

الـــخُـــلاصـــة

تـم تحقيـق المقـاطع العرضـية للتشـتت الإلكتـرون التفاضـلي بواسـطة جزيئـات الأمونيـا والفوسفين من ١٥ فولت إلـى ٥٠٠ فولت و ٥ فولت إلـى ٥٠٠ فولت علـى التـوالي. تـم إجـراء الحسابات المطلوبة باستخدام أشكال موجية جزئية تميز الجزيء المستهدف ومركز هارتري-فوك للوظـائف الجزيئيـة. توضـح النتـائج مـن هـذا النمـوذج أهميـة التبـادل ، وكـذلك مسـاهمات الارتباط والاستقطاب ، لا سيما في زوايا التشتت المنخفضة والطاقة العارضة ، لأن الإمكانـات المستخدمة تحتوي على جزء ثابت - يتم إنشاؤه رقميًا من خلال الحوسبة الكمومية. تـم اكتشـاف توافـق جيـد بـين المقـاطع العرضـية التفاضـلية المحسـوبة وقاعـدة بيانـات واسـعة مـن البيانـات التجريبية. تم تحليل زوايا التشتت الكروية المختلفة ونطاقات الطاقة في هذا البحث.

1. INTRODUCTION

Electron-particle collisions are important in understanding and characterizing plasmas, in addition to biological and astrophysical environments that involve molecules [1-6]. The electron scattering of two identical molecules, ammonia NH_3 and phosphine, is investigated in this study PH_3 . Both compounds have significant roles in several scientific fields. Plasma catalysis, which is used in the chemical industry, necessitates knowledge of the impact of the electron on the scattering cross sections of ammonia [7]. There, NH_3 is commonly utilized to produce nitride films, as a nitrogen supply, and so on. Nitrogen compounds [8], in addition to its use in plasma, ammonia is an essential source of nitrogen in the human body and a crucial building block of proteins. Glutamate dehydrogenase may convert ammonia into glutamate, an amino acid, directly[9]. The fact that NH_3 can be easily compressed makes it a promising candidate for research into carbon-free energy transmission, storage, and generation in the future generation of systems[10]. Jupiter and Saturn's atmospheres include condensable volatiles NH_3. Thus, cross-sectional electron scattering measurements of NH_3 are urgently required for understanding interstellar processes and simulating such planetary atmospheres. Phosphine PH_3 is a very poisonous and combustible gas used in the production of photovoltaic cells [12], and it is one of the most significant phosphorus species identified in astronomical contexts, such as the circumstellar disc [11] and Saturn's atmosphere. Results from the electrical PH_3 cross-sectional impact experiment are essential for advancing our knowledge of the chemistry of phosphorus in space. Results from a literature search on elastic electron scattering by NH_3 and PH_3 molecules are as follows. Numerous reports of experimental and theoretical research have been made [5]. However, the most majority of only exist in the low incident electron energy area, whereas the numbers diminish at intermediate and high energies [13]. Few research have been published on the topic. Alle et al. [14] evaluated the differential cross-sections (DCS) and momentum transfer cross-sections (MTCS) of an electron scattering from NH_3 in the low energy band of 2-30 eV using a cross-electron molecular beam. The elastic scattering cross-sections were recently measured by Homem and colleagues using proportional flow technology and 50-500 volts. Besides , M. Homem et al.[15] published their estimates for Differtional, momentum, and total cross section based on their experimental findings employing a single center expansion (SCE) Methods for incoming electron energies between 1 and 500 eV were merged with the Pade method. Yuan and Zhang [16] derived DCS, MTCS, and TCS values in the 0.5-20 eV energy range using spherical molecule wave functions in the first-order Born approximation. Using the multichannel Schwinger approach, Winsted et al. [17] determined DCS for PH_3.

One can expect incoming electron energies between 1 and 40 eV Similarly, M.Lima,et al. [18] used the Schwinger multichannel approach; they maintained constant pseudo-potential parameters and produced DCS in the 10-30 eV power range. The DCS and MTCS were calculated by Z. Zhang [19] for energies between 0.1 and 50 eV using a spherical molecule wave function. DCS is calculated for energies between 10 and 20 keV by Aouchiche and Medegga [20] using partial wave stretching with spherical potentials. Kaur et al [21] . Using a spherical complex optical voltage technique is done in nuclei with a fixed approximation. Both NH3 and PH_3 particles have been reported to exhibit theoretical DCS up to 30 eV, MTCS up to 100 eV, and TCS up to 100 eV. New theoretical and experimental results and data for MTCS and TCS up to 500 eV were recently evaluated and suggested by Itekawa[22]. Theoretical work has progressed to the point of experimentation. Only TCS data

were collected for electron scattering, however NH_3 and PH_3 were used as scattering targets. TCS values for NH_3[23] between 1 and 100 eV and PH_3[24] between 0.5 and 370 eV were calculated by Szmytkowski et al. using a linear transfer approach. [25] Wrote to the editors to provide comparable experimental data on electron-NH_3 scattering at energies between 75 and 400 eV. Even then, there are no empirical save the aforementioned theoretical calculations and TCS observations. Scattering cross sections for electrons in PH_3 have been reported.

In this work, we describe the results of an investigation into the electron scattering of NH_3 and PH_3. There is a large variation in the incident energy of different particles. Take a visual potential model approach. Our chemical is utilized in combination with the partial wave phase shift analysis to characterize the scattering mechanism. A fixed potential, exchange, polarization, and absorption all contribute to the optical potential. For a solution to the Schrodinger problem, the partial Waveform analysis technique is used [26-28]. By using the dispersion phase shifts provided by the found solutions, we may derive the findings of the different cross sections. We apply the standard optical potential approach, which has been employed extensively in previous investigations of electron scattering. Almost majority of these computations require the selection of an experimental model potential other than the static potential[5], which may include exchange, polarization, or absorption. The elastic scattering of electrons with NH_3 and PH_3 has been investigated using this method. The reliability of this method is influenced by the available visual possibilities. It's challenging to determine the polycentric target molecule's static potential from an expelled electron.[29]

The scattering process is further described by the independent atom model, which specifies the simplest method for each atom in a molecule to interact with an expelled electron. The metacentric molecular potential has been obtained by a number of alternative approaches. In order to increase the size of molecular orbital wave functions, SCE [27] is commonly employed. With relation to the molecular core of a polymer. The molecule's wave function was calculated of Hartree-Fock. One of our primary goals is to establish a method to calculate the constant electron scattering potentials of NH_3 and PH_3 so that it can be tested, and so that our DCS, MTCS, and TCS can be compared with current comprehensive results. Since the wave functions and outgoing potential are presented analytically [30], we used standard and widely tested expressions for other energies and the exchange, polarization, and absorption components of the complex optical potential.

2. Theoretical model

"The Calculations the differential cross section dσ (Ω)) / dΩ have been developed in coplanar geometry using partial waveforms and the non-relativistic approach, where is the solid. The scattering angle of electrons. In these circumstances dσ (Ω))/dΩ can be given by the square of the scattering amplitude f (θ) while"

$$\boldsymbol{f(\theta) = \frac{1}{K}\sum_{t=i}^{\infty}(2+1)e^{i\delta i}\, sin\, \delta_i p_i(cos\theta)} \quad (1)$$

"k is related to kinetic energy. E by 2E = k^2 , 1the kinetic momentum's quantum number, $P_l(\cos\theta)$ the Legendre polynomial and δ_l is the phase shift induced by the spherical potential V (r) in the outgoing wave relatively to the free wave (for more details see Ref.[31]). NH_3 being a pyramidal molecule with a heavy atom N, the charge distribution can be assumed as a spherical molecule centered at the nucleus N. Under these assumptions, the total potential V (r) may be approximated by a spherical one including the static potential $V_{st}(r)$ and the two fine effects called polarization potential, $V_p(r)$, and exchange potential, $V_{ex}(r)$"

$$\mathbf{V(r) = V_{st}(r) + V_p(r) + V_{ex}(r)} \quad (2)$$

$$\mathbf{V(r) = V_{st}(r) + V_{ex}(r) + V_{cor}(r) + V_{pol}(r)} \quad (3)$$

"Between the projectile and the target atom, the electrostatic interaction's energy is determined.[32] For a resting mass projectile m_0 moving in central field V(r) with a velocity V, the relativistic Dirac equation [18] is given by"[33]

$$[\mathbf{c\alpha}.\mathbf{p} + \boldsymbol{\beta}\mathbf{m_0c^2} + \mathbf{V(r)}]\boldsymbol{\psi}(\mathbf{r}) = \mathbf{E}\boldsymbol{\psi}(\mathbf{r}) \quad (4)$$

Where $\boldsymbol{E^2 = P^2C^2 + m_o^2C^4}$ "the total energy"

$$= \boldsymbol{E_1 + m_o^2C^4}$$

"c is speed of light in vacuum, E_i is the incident particle's kinetic energy, α and β are the standard 4 x 4 Dirac matrices".

$$\mathbf{V_{st}(r)} = \mathbf{Z_o e\varphi(r)} = \mathbf{Z_o e[\varphi_n(r) + \varphi_e(r)]} \quad (5)$$

$$\mathbf{V_{st}(r)} = \mathbf{Z_o e\varphi(r)} = \mathbf{Z_o e[\varphi_n(r) + \varphi_e(r)]} \quad (6)$$

$$\emptyset(\mathbf{r}) = \emptyset_{\mathbf{e}}(\mathbf{r}) + \emptyset_{\mathbf{n}}(\mathbf{r}) \quad (7)$$

$$\emptyset_e(\boldsymbol{r}) = -\boldsymbol{e}\left[\frac{1}{r}\int_0^{\mathbf{r}} \mathbf{4\pi r`^2}\,\boldsymbol{\rho}_{\mathbf{e}}(\mathbf{r`})\mathbf{dr`} + \int_{\mathbf{r}}^{\infty} \mathbf{4\pi r`}\,\boldsymbol{\rho}_{\mathbf{e}}(\mathbf{r`})\mathbf{dr`}\right] \quad (8)$$

$$\emptyset_n(\boldsymbol{r}) = \boldsymbol{e}\left[\frac{1}{r}\int_0^{r} \mathbf{4\pi r`^2}\,\boldsymbol{\rho}_{\boldsymbol{n}}(\boldsymbol{r`})\boldsymbol{dr`} + \int_{\mathbf{r}}^{\infty} \mathbf{4\pi r`}\,\boldsymbol{\rho}_{\mathbf{n}}(\mathbf{r`})\mathbf{dr`}\right] \quad (9)$$

where Z_0 e is the charge of the electrons being shot at (Z_0 = -1), (r) is the electrostatic potential of the molecule being shot at, and (r) is the electrostatic potential function of the target atom, expressed as the sum of contributions from the nucleus and the electron cloud, n(r) and e(r), respectively, formed by the distribution of electric and nuclear charge on a straight[34]. In this investigation, the Fermi nuclear charge distribution _n(r) supplied by Hahn et al.[35] is employed to derive$\emptyset_{\,n}$. (r). However, it has produced $\emptyset_e$ (r) by making use of the most accurate electron densities $\emptyset_e$ (r) for free atoms, as calculated by self-consistent relativistic Dirac-Fock (DF) calculations [36]. Density e is also used in the same way to get the electron exchange potential (r). The Furness and McCarthy[37] model of exchange potential. The calculations presented in this study rely on a locally approximated version of the exchange interaction provided by:

$$\boldsymbol{V_{ex}(r) = \frac{1}{2}\left(E_i - V_{st}(r)\right) - \frac{1}{2}\left[(E_i - V_{st}(r))^2 + 4\pi a_o e^4 \rho_e(r)\right]^{1/2}}$$

(10)

Where E_i is the kinetic energy of the bullet and a_0 is the initial Bohr radius for the binding and polarization potentials, the parameter-free polarization potential the binding energy of the target molecule determines V_{cpol}(r). It comes in two sections: short-running V_{cor}(r) portions and long-running $V_{\,pol}$(r) parts, and it's offered by[34].

$$\mathbf{V_{cpol}(r)} = \begin{cases} \mathbf{V_{cor}} & \mathbf{if} \quad \mathbf{r < r_c} \\ \mathbf{V_{pol}} & \mathbf{if} \quad \mathbf{r \geq r_c} \end{cases} \quad (11)$$

In the present work, we adopted the parameterization of the correlation potential given by J.K. O'Connell and N. F. Lane[38]

$$2v_{\,c}\,[\rho] \equiv \begin{cases} 0.0622 ln r_s - 0.096 + 0.018 r_s ln r_s - 0.02 r_s & r_s \leq 0.7 \\ -0.1231 + 0.03796 \ln r_s\,, 0.7 < r_s \leq 10 \\ -0.876 r_s^{-1} + 2.65 r_s^{-3/2} - 2.8 r_s^{-2} - 0.8 r_s^{-5/2}\,, \; 10 \leq r_s \end{cases} \quad (12)$$

Where

$$\mathbf{r_s} = \left(\mathbf{3}/\mathbf{4\pi\rho}\right)^{\mathbf{1}/\mathbf{3}} \quad (13)$$

A static potential is produced as a result of the projectile's electrostatic interaction with the distribution of atomic charge. The Dirac-Focus electrons density[35] and the nuclear charge distribution of Fermi [39] are used to produce this static potential. The current work employs Furness and McCarthy's [37] quasi-classical local exchange potential, which is constructed from non-local exchange interactions utilizing WKB-like wave functions. The potential for polarization occurs as a result of the displacement of the atom's charges by the charged event and remains attractively ejected to both electrons. This is formed from non-local exchange interactions with WKB-like wave functions Polarization occurs as a result of the displacement of the atom's charges by the charged event and stays favorably ejected to both electrons. Following sulfate [40] , this

research use the $V_{cp}(r)$ global correlation-polarization potential, which blends parameter-free long range Buckingham potentials with short range correlation potentials based the local density approximation . The particle loss in the different inelastic channels beyond which the inelastic threshold opens is calculated using the negative imaginary part—$iW_{abs}(r)$. V_{st} (r), V_{ex} (r), V_{cp} (r), and $W_{abs}(r)$ components are shown in detail elsewhere [41-43] . The elastic scattering amplitude completely describes the scattering of electrons by the potential V(r) in the Dirac partial-wave analysis [44, 45] . It is made up of two contributions: spin-conserving (direct) contribution f (Θ) and the spin-flip contribution g(Θ). The DCS elastic of an initially unpolarized electron is computed. as follows:

$$\frac{d\sigma}{d\Omega} = |f(\theta)|^2 + |g(\theta)|^2 \quad (14)$$

For e- PH_3, NH3 scattering, the partial wave technique cannot be utilized directly to obtain observable quantities because the interaction between the projectile and the molecule is not spherically symmetric. Direct and spin-flip scattering amplitudes are calculated as[42]:

$$F(\theta) = \sum_i \exp(iq.r_i) f_i(\theta) \quad (15)$$

And

$$g(\theta) = \sum_i \exp(iq.r_i)\, g_i(\theta) \quad (16)$$

"where iq is the momentum transfer and r_i is the position vector of an atom i's nucleus with reference to an arbitrary origin .where $f_i(\theta)$ and $\mathbf{g_i(\theta)}$ are the amplitudes of scattering of the element's component-free atom. The appropriate DCS is calculated by averaging the orientations of all randomly oriented particles and is denoted by"

$$\frac{d\sigma}{d\Omega} = \langle |F(\theta)|^2 + |G(\theta)|^2 \rangle \quad (17)$$

$$= \sum_{i,j} exp(\mathbf{iq}.\mathbf{r_{i,j}}) [f_i(\theta) f_j^*(\theta) + g_i(\theta) g_j^*(\theta)] \quad (18)$$

$$= \sum_{i,j} \frac{sin(qr_{ij})}{qr_{ij}} [\mathbf{f_i}(\theta) \mathbf{f_j^*}(\theta) + \mathbf{g_i}(\theta) \mathbf{g_j^*}(\theta)] \quad (19)$$

$$= \sum_i [|f_i(\theta)|^2 + |g_i(\theta)|^2] + \sum_{i \neq j} \frac{sin(qr_{ij})}{qr_{ij}} [f_i(\theta) f_j^*(\theta) + g_i(\theta) g_j^*(\theta)] \quad (20)$$

In this equation, q = 2k sin(θ/2), r_{ij} is distance between the i-th & j-th atoms, $\sin(qr_{ij})/qr_{ij} = 1$ when $qr_{ij} = 0$, and the expression $\sum_{i \neq j}$ reflects the contribution of interference to the molecular DCS. The integrated elasticσ_{el}el, momentum-transferσ_m, and viscosity v cross-sections for e – PH_3, NH_3 scattering are expressed in terms of the DCS as

$$\sigma_{el} = \int \frac{d\sigma}{d\Omega} d\Omega = 2\pi \int_0^\pi \left(\frac{d\sigma}{d\Omega}\right) \sin(\theta)\, d\theta \quad (21)$$

$$\sigma_m = 2\pi \int_0^\pi (1 - cos\theta) \left(\frac{d\sigma}{d\Omega}\right) \sin(\theta) d\theta \quad (22)$$

$$\sigma_v = 3\pi \int_0^\pi [1 - (cos\theta)^2] \left(\frac{d\sigma}{d\Omega}\right) \sin(\theta) d\theta \quad (23)$$

"The total cross-section for both projectiles may be calculated using the following expression":

$$\sigma_{tot} = \frac{4\pi}{k} \sum_i \mathbf{lmf_i}(\mathbf{0}) \quad (24)$$

In this case, Imfi(0) represents the imaginary part of the I atom's forward direct scattering amplitude, which is zero. Due to the fact that the elastic and inelastic (absorption) components are all included in the imaginary component, tot. In this study, we express the inelastic cross-section in terms of.

$$\sigma_{inel} = \sigma_{tot} - \sigma_{el} \quad (25)$$

The main problem with the voltage that is does not explain the multiple scattering of the shells from atoms of the molecule components, which limits its applicability at relatively high energies (>100 eV) [42, 46]. Another reason for the failure of the low-energy models its lack of knowledge of the mutual interference between adjacent atomic cross sections. To address this issue, F. Blanco [44]. presented si-correction assay ($0 \leq s_i \leq 1$) for i-th molecule and j-th atoms, which is provided by:

$$"s_i = 1 - \frac{\varepsilon_i^{(2)}}{2_i} + \frac{\varepsilon_i^3}{3_i} - \frac{\varepsilon_i^4}{4_i} + \cdots \mp \frac{\varepsilon_i^N}{N_i}" \quad (26)$$

Where

$$\boldsymbol{\varepsilon_i^{(m)} = \frac{N-m+1}{N-1}\sum_{i\neq j}\frac{\sigma_{j\varepsilon_j^{(m-1)}}}{\alpha_{ij}}\ (m = 2, \dots, N)}\ (27)$$

"Represents overlapping m - atoms N is the number of atoms the target molecule, and ij = max($4r\pi r^2, \sigma_i\sigma_j$) where i and j are atomic total cross-sections of molecule's i-th and j-th atoms". Equation (16) has the following form for NH_3 and PH_3molecule (N = 4)

These things lessen the impact that individual atoms have on the cross-section of the molecule. $\boldsymbol{s_i = 1 - \frac{\varepsilon_i^{(2)}}{2!} + \frac{\varepsilon_i^{(3)}}{3!}}$ (28)

. Blanco et al. [46] enhanced the formalism by introducing a new factor v_{ij} ,to the positive values of

$\sum_{i\neq j} v_{ijs_is_j}\ \frac{\sin(qr_{ij})}{qr_{ij}}\left[f_i(\theta)f_j^*(\theta)\right]$, Which is defined as

$v_{ij} = r_{ij}^2/\left(r_{ij}^2 + \rho_{ij}^2\right)$,with a length-dimensional parameter

$\rho_{ij} = \max\left(\frac{\sqrt{\sigma_i}}{\pi}, \frac{\sqrt{a_j}}{\pi}, \frac{1}{k}\right)$. Here, ($\sqrt{\sigma/\pi}$) depicts the radius of an area circle As a result, Equation[47] has been screening-corrected

$$\left(\frac{d\sigma}{d\Omega}\right)^s = \sum_i s_i^2\ [|f_i(\theta)|^2 + |g_i(\theta)|^2] + \sum_{i\neq j} v_{ij}s_is_j\frac{\sin(qr_{ij})}{qr_{ij}}\left[f_i(\theta)f_j^*(\theta) + g_i(\theta)g_j^*(\theta)\right] \quad (29)$$

"The screening-corrected integrated elastic σ^s_{el} , momentum-transfer σ^s_m , viscosity σ^s_v , and total σ^s_{tot} cross-sections are given by"

$$\sigma_{el}^s = 2\pi\int_0^\pi\left(\frac{d\sigma}{d}\right)^s\sin(\theta)d(\theta) \quad (30)$$

RESULTS :

We have used an optical model potential to do a relativistic calculation of the Total Cross Section (TCs), Differential Cross Section (DCs), and momentum transfer for electrons for NH_3 and PH_3 over a wide range of energies (15-500 eV). Both actual and absorption potentials were included in our estimate. For e-NH_3 collision

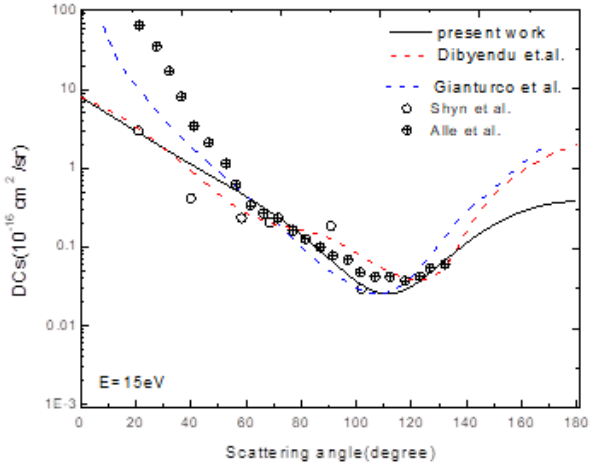

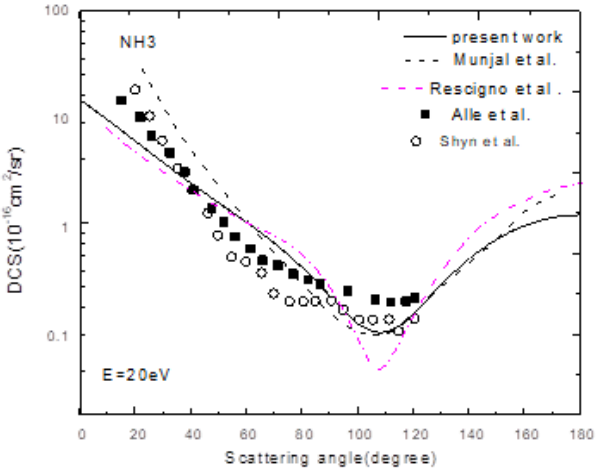

In figure .(1) we compared our results of DCs at 15 eV with theoretical data of Dibyendu .[5],Gianturco .[48] and the experimental data with Alle et al.[49],Shyn.[50], and for the energy 20eV,our results compared with the delta Dibyendu et al.[5],Manjal et al.[51], Rescigno[52] and the measurements of Alle et al.[14], Shyn et al.[50], for the energy 30eV,our results compared with the delta Dibyendu et al.[5],Sali et al.[53], and the measurements of Alle et al.[14],Homem etal.[15], for the energy 50eV,our results compared with the delta Dibyendu et al.[5], Homem etal.[15] and the measurements of Homem etal.[15]

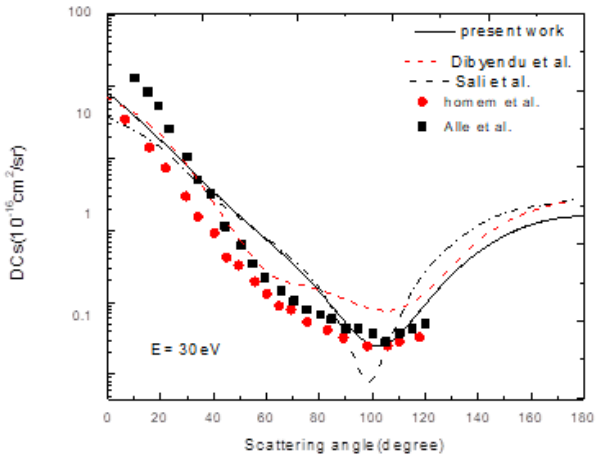

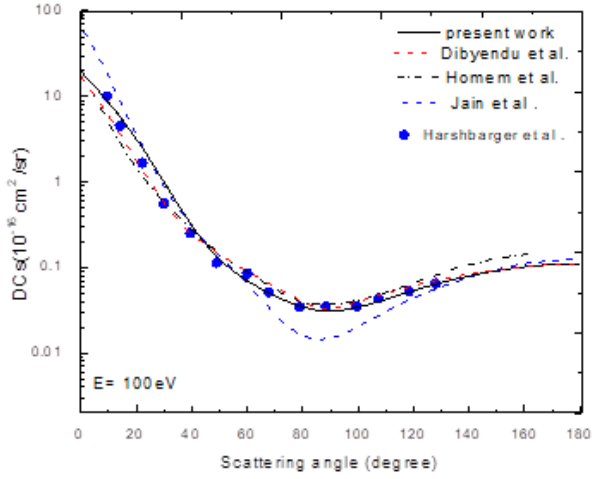

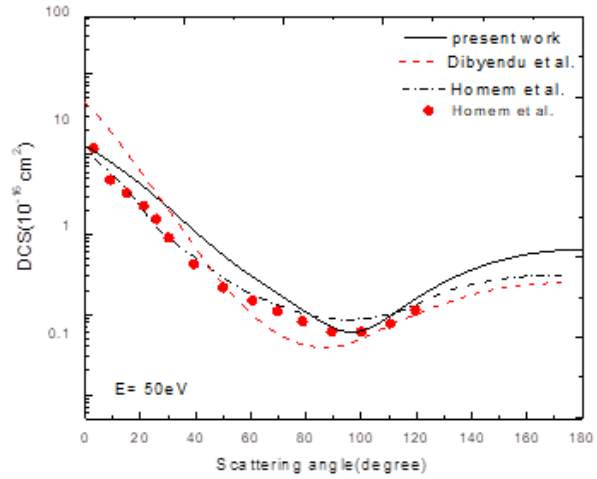

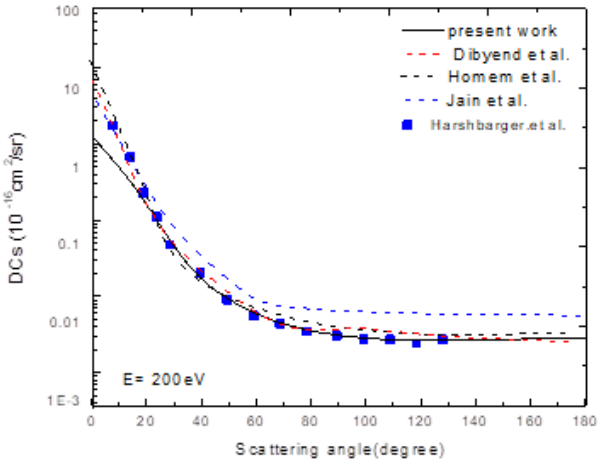

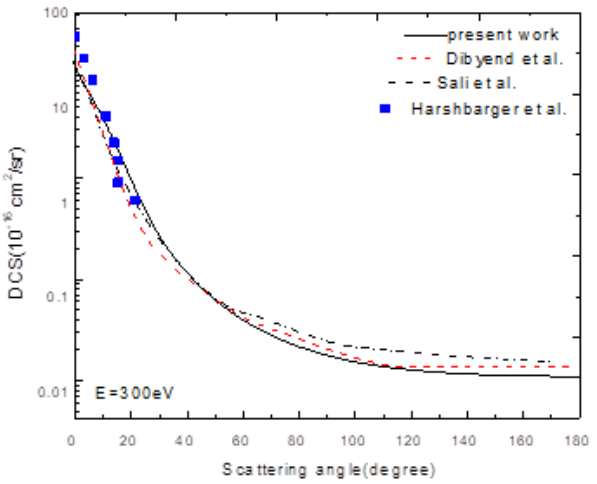

"Figure(1) . DCS (cm^2 /sr) for elastic scattering of electrons of ammonia in energies of 15, 20", 30, and 50 eV. Theoretical: Dibyendu [5] ,Gianturco[48],Manjal[51],Rescigno[52],Sali[53] and Homem [15] Experimental:Shyn[50],Alle[49],Alle[14]and Homem[15].

Comparisons of our results for DCs at 100 and 200 eV with theoretical data from Dibyendu et al.[5], Homem et al.[15], Jain et al.[54], and measurements from Hershberger et al.[55] and Homem et al.[15] and for the energy 300eV, our results compared with the delta Dibyendu et al.[5], Sali et al.[53] and the measurements of Hershberger et al.[55], and for the energy 400eV,our results compared with the delta Dibyendu et al.[5] and the measurements Homem et al.[15] . can be seen in fig.(2).

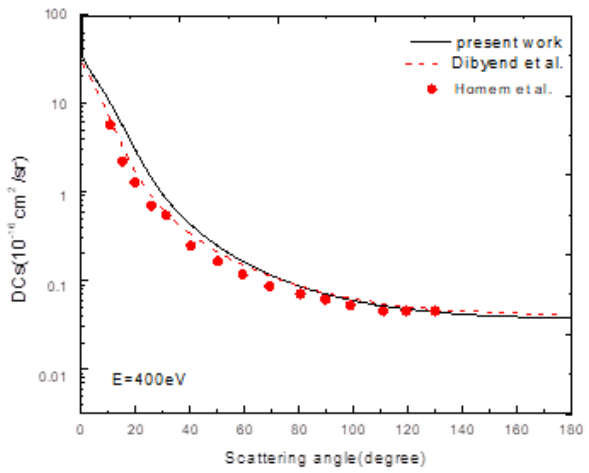

"Figure (2) . DCS (cm^2 /sr) for elastic scattering from electrons of ammonia at energies of 100, 200, 300, & 400 eV. Theoretical: Dibyendu [5] , Sali[8] , jain [56]and Homem[47] .Experimental: Harshbarger [55]and Haque et al.[47]".

In figure.(3) we compared our results of DCs at 500 eV with the theoretical data of Dibyendu et al.[5], Sali et al.[53] and measurements of Hershberger et al.[55].

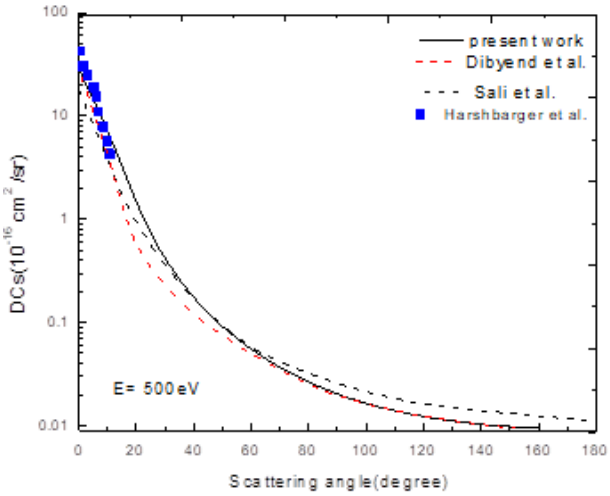

In figure.(4a) we compared our results of TCS with the theoretical data of Jain et al[56] and the measurements of Zecca et al.[25] ,Sueok et al.[57].In fig.(4b) we compared our results of TMCS with the theoretical data of Dibyendu et al.[5] and the measurements Homem etal.[15],Alle et al.[14],Gianturco et al.[48].

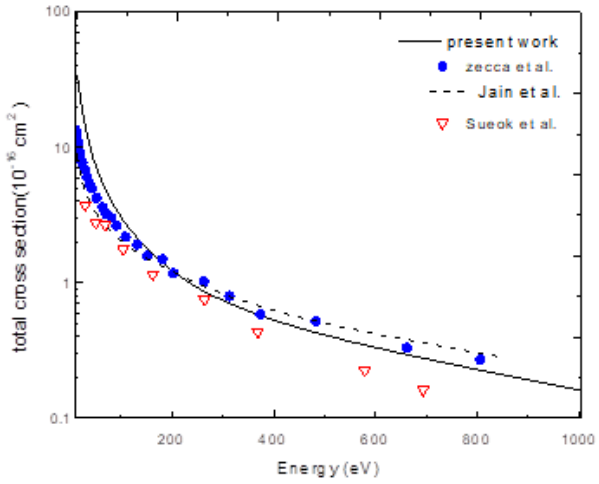

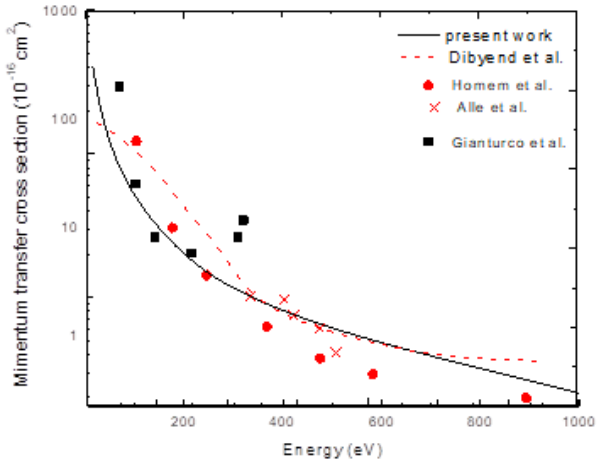

"Figure 4: TCS and MTCS for the elastic scattering of electrons from NH3. Theoretical data for Dibyendu [5] Jain [56] Experimental data for Zecca[25]"

"Figure 5 shows the DCs results of e-PH_3 collision at 5 eV with that compared by the theoretical data of Kaur et al.[21] and the results also compared with the experimental data of Jianmin et al.[19]. For the energy of 10 eV, the results were comparison with the data of Dibyendu et al.[5], Kaur et al.[52] and the results also compared with the experimental data of Jianmin et al.[53]. For the energy of 15 and 20 eV, these results were compared with the data of Dibyendu et al.[5], Kaur et al.[52],Battega et al[18] and the results also compared with the experimental data of Jianmin et al".[53].

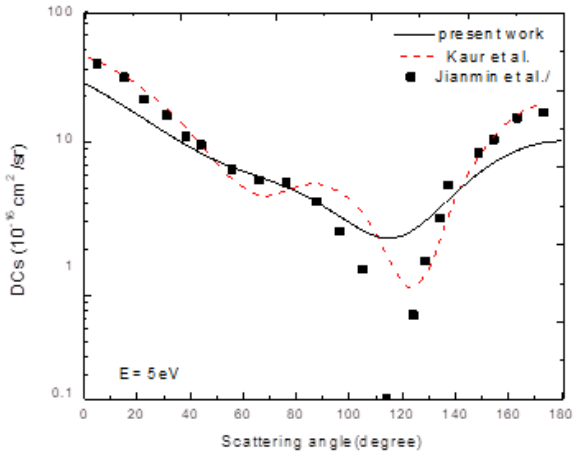

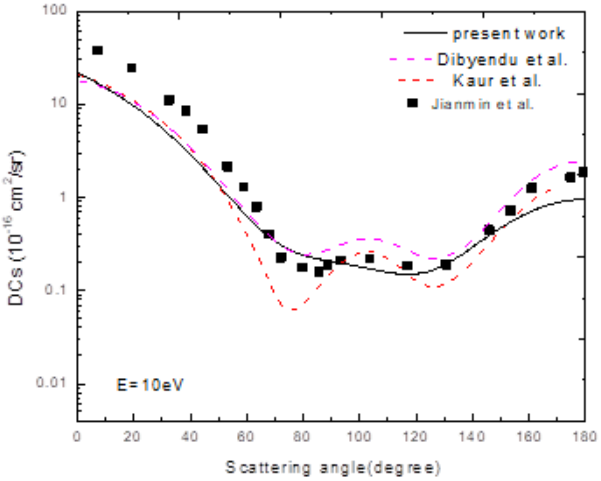

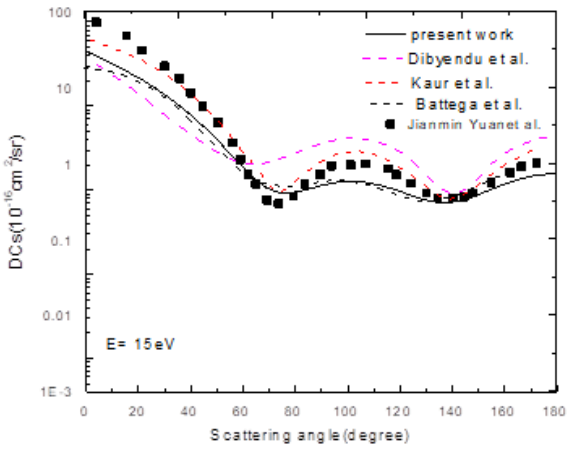

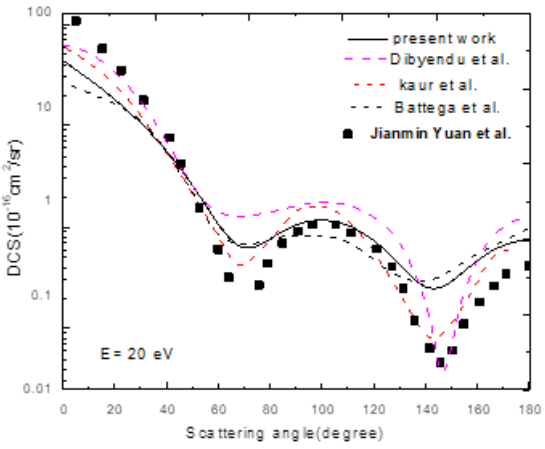

"Figure(5) . DCS (cm^2 /sr) for elastic scattering of electrons from PH3 at energies 5, 10, 15, and 20 eV. Theoretical: Kaur[21], Dibyendu [5],battega[18], Experimental:Jianmin"[19]

Results from DC simulations of e-PH_3 collisions at 25 eV are shown in Figure 6 and compared to theoretical data from Battega et al.[54] and experimental data from Sali et al.[53]. The findings were compared to those found by Dibyendu et al.[5], Rescigno et al.[52], and Battelega et al.[54] at an energy of 30 eV. Comparisons were made between the results and the data of Dibyendu et al.[5], Jianmin et al.[53], and "Jianmin et al experimental .'s data at an energy of 50 eV. .[53] The findings were compared to those found by Dibyendu et al.[5] and Aouchiche et al.[6] with an energy of 100 eV". .[20].

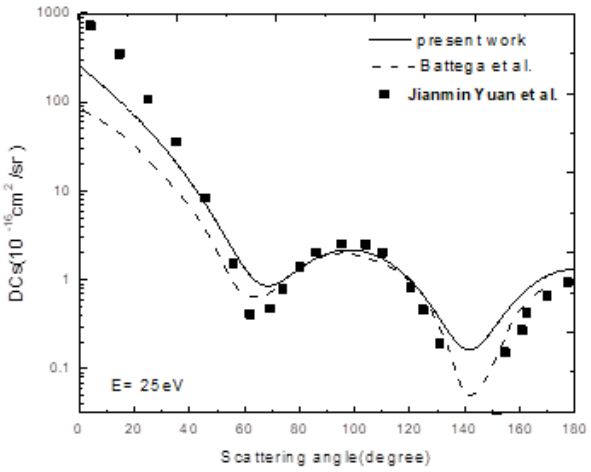

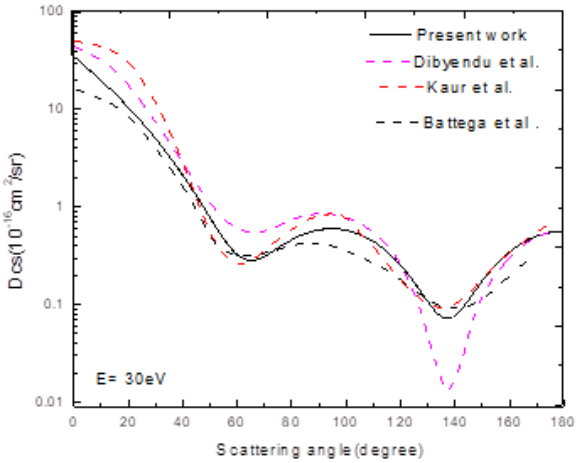

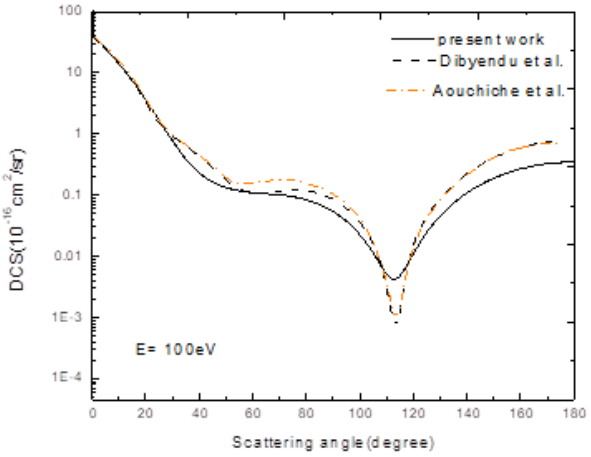

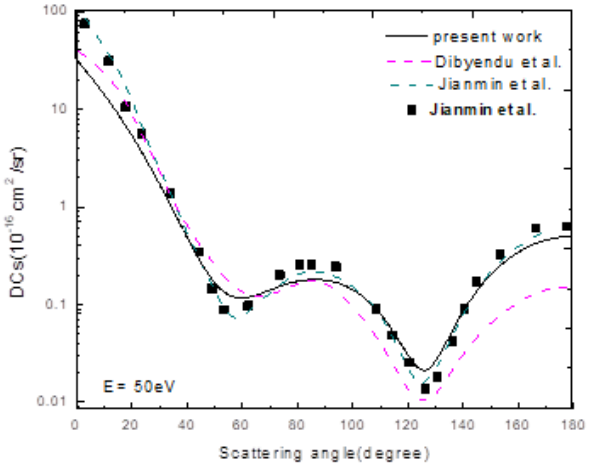

"Figure 6: DCS (cm^2 /sr) for elastic scattering of electrons from PH_3 at energie 25,30,50,and"

100eV. Theoretical :Kaur[52], Dibyendu [5],battega[54],Aouchiche [20]and Jianmin[53] Experimental: Jianmin[53]

"Figure 7 shows the DCs results of e-PH_3 collision at 200, 400 eV with that compared by the theoretical data of Dibyendu et al.[5]. For the energy of 300,500 eV, the results were compared with the data of Dibyendu et al.[5],and Aouchiche et al"[55].

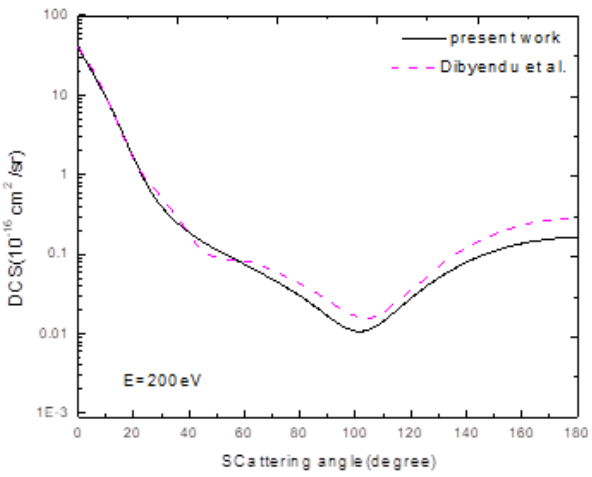

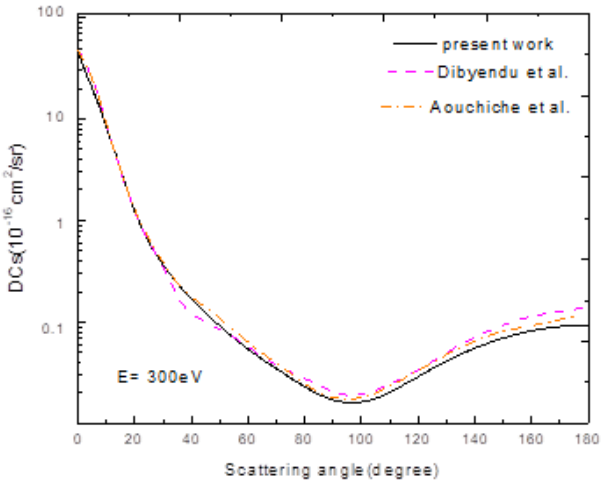

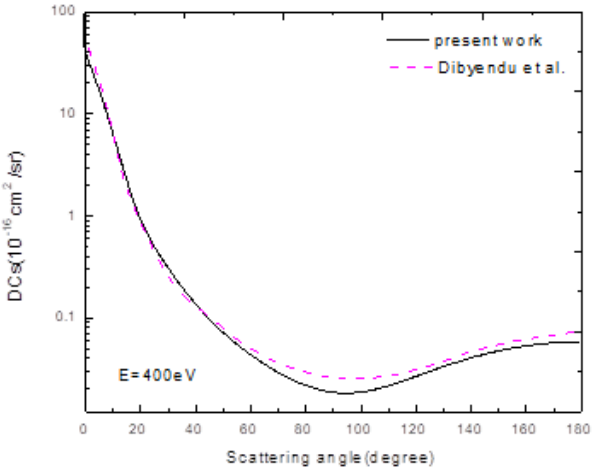

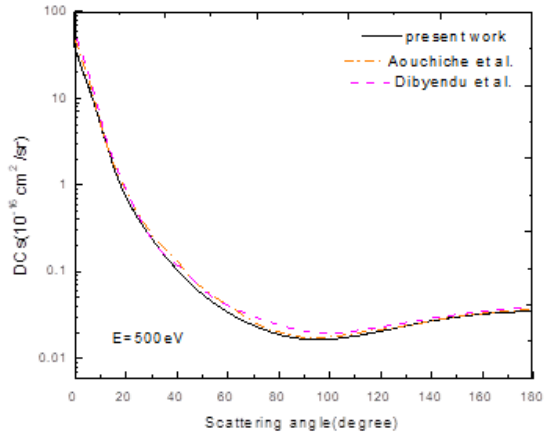

"Figure 7:DCS (cm^2 /sr) the elastic scattering of electrons from PH3 at energies 200, 30, 400, &"

500eV. Theoretical: Kaur[52], Dibyendu [5], and Aouchiche [55]

TCS results are discussed and compared to theoretical data in Fig. 8a. We compared our findings to those of Dibyendu and Kaur [5, 52], "as well as to the experimental data of Szmyikaw et al". [24]. "Figure 8b compares the experimental data of TMCS with the theoretical data of Dibyendu".[5], Kaur et al.[52], and Winstend et al.[54].[17].

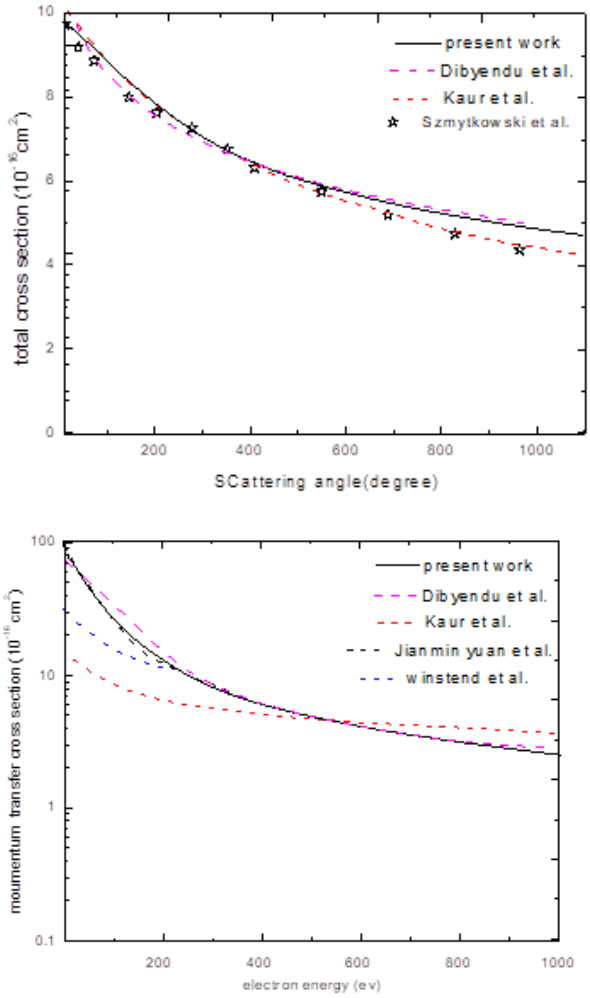

"Figure 8: TCS and MTCS for the elastic scattering of electrons from PH3. Theoretical data for Dibyendu" [5], Kaur[52],Jianmin[19] and Winstend[17], Experimental: Szmytkowski[24].

Discussion and Conclusion

The electron scattering of NH_3 and PH_3 molecules is investigated in depth in this paper. Mesoscale spherical complex potentials were constructed with the stabilization, exchange, polarization, and absorption potentials. For electron impact energies up to 500eV, findings for DCSs, TCSs, and M CSs are provided. We observed usually excellent agreement between our cross-sections and both experimental data and previous theoretical NH_3 electron scattering results.The present study's absorption voltage, which is above 30 V, produces excellent findings. The electron scattering cross section of PH_3 has not been reliably measured. Our results for PH_3 are easily corroborated when compared to other theoretical calculations and to good electron scattering measurements for NH_3. Theoretical estimations of electron scattering from the PH_3 molecule require experimental confirmation. At the moment, we have successfully used our approach, which is based on well-established analytical skills, to characterize the collision of an elastic electron with NH_3 and PH_3. More complicated compounds are within the scope of this method. Our technique, which makes use of static analytical capabilities, accurately describes the collision of the elastic electron with NH_3 and PH_3, providing support "for the theoretical predictions of electron scattering from the PH3 molecule" that have been performed thus far. The scattering angles and power bands studied here can be applied to particles with more complicated shapes.

In general,

1. the results obtained from DCs for the collision of e-NH_3 and PH_3 with different energies are fully consistent with those obtained by researchers in theoretical and practical fields.
2. regarding the results of e-PH_3 no practical results were obtained for high energies to compare with them only the theoretical and it was compatible with the readings of others

at medium and high energies, the results obtained are improved.

3. according to the overall results and momentum transfer shown in the two figures at 4 and 8, the results for the strengths (TCs) appeared to be good except for the higher energies where some inconsistency was observed in the MTCs.
4. We have seen some concavities be consoled to the weakness in the potential field of the collision in most DCS figures at low energies, but not in the figures at high energies.

REFERENCES

[1] Bartschat, K. and M.J. Kushner, Electron collisions with atoms, ions, molecules, and surfaces: Fundamental science empowering advances in technology. Proceedings of the National Academy of Sciences, 2016. 113(26): p. 7026-7034.https://doi.org/10.1073/pnas.1606132113

[2] Mahato, D., et al., Electron impact ionisation cross section for organoplatinum compounds. Molecular Physics, 2016. 114(21): p. 3104-3111.https://doi.org/10.1080/00268976.2016.1219408

[3] Schippers, S., et al., Roadmap on photonic, electronic and atomic collision physics: II. Electron and antimatter interactions. Journal of Physics B: Atomic, Molecular and Optical Physics, 2019. 52(17): p. 171002.https://doi.org/10.1088/1361-6455/ab26e0

[4] Mason, N., The status of the database for plasma processing. Journal of Physics D: Applied Physics, 2009. 42(19): p. 194003. https://iopscience.iop.org/article/10.1088/0022-3727/42/19/194003/meta

[5] Mahato, D., L. Sharma, and R. Srivastava, An approach to study electron and positron scattering from NH3 and PH3 using the analytic static potential. Journal of Physics B: Atomic, Molecular and Optical Physics, 2020. 53(22): p. 225204.https://doi.org/10.1088/1361-6455/abb9f4

[6] Khalf, A.A., Calculating the Atomic electron impact Ionization Cross Section for some elements. Journal Of Wassit For Science & Medicine, 2008. 1(2).https://www.iasj.net/iasj/download/9f969de821ca6e86

[7] Body, T., et al., A volume-averaged model of nitrogen–hydrogen plasma chemistry to investigate ammonia production in a plasma-surface-interaction device. Plasma Physics and Controlled Fusion, 2018. 60(7): p. 075011. https://doi.org/10.1088/1361-6587/aab740

[8] Egert, P., et al., Mass Spectrometry Study of Ammonia Formed During Plasma Nitrocarburizing and Nitriding Processes. Materials Research, 2018. 21.https://doi.org/10.1590/1980-5373-MR-2018-0133

[9] Spinelli, J.B., et al., Metabolic recycling of ammonia via glutamate dehydrogenase supports breast cancer biomass. Science, 2017. 358(6365): p. 941-946.https://doi.org/10.1126/science.aam9305

[10] Valera-Medina, A., et al., Ammonia for power. Progress in Energy and combustion science, 2018. 69: p. 63-102.https://doi.org/10.1016/j.pecs.2018.07.001

[11] Agúndez, M., et al., Confirmation of circumstellar phosphine. The Astrophysical journal letters, 2014. 790(2): p. L27.https://doi.org/10.1088/2041-8205/790/2/L27

[12] Fthenakis, V. and P. Moskowitz, Characterization and control of phosphine hazards in photovoltaic cell manufacture. Solar cells, 1987. 22(4): p. 303-317.https://doi.org/10.1016/0379-6787(87)90060-3

[13] Hassan, R.M.A. and A.A. Khalaf, Atomic Lithium Excitation by Electron Impact. Journal of Kufa-Physics, 2019. 11(02).https://doi.org/10.1016/0379-6787(87)90060-3

[14] Alle, D., et al., Elastic scattering of low-energy electrons from ammonia. Journal of Physics B: Atomic, Molecular and Optical Physics, 1992. 25(7): p. 1533.https://doi.org/10.1088/0953-4075/25/7/023

[15] Homem, M., et al., Electron collisions with ammonia and formamide in the low-and intermediate-energy ranges. Physical Review A, 2014. 90(6): p. 062704.https://doi.org/10.1103/PhysRevA.90.062704

[16] Yuan, J. and Z. Zhang, Low-energy electron scattering with H 2 O and NH 3 molecules. Physical Review A, 1992. 45(7): p. 4565.https://doi.org/10.1103/PhysRevA.45.4565

[17] Winstead, C., Q. Sun, and V. McKoy, JL d. S. Lino, and MAP Lima. Z. Phys. D, 1992. 24: p. 141.

[18] Bettega, M., M. Lima, and L. Ferreira, Cross sections for collisions of low-energy electrons with the hydrides PH3, AsH3, SbH3, SnH4, TeH2, and HI. The Journal of chemical physics, 1996. 105(3): p. 1029-1033.https://doi.org/10.1063/1.471947

[19] Yuan, J. and Z. Zhang, Electron scattering with H2S and PH3 molecules. Zeitschrift für Physik D Atoms, Molecules and Clusters, 1993. 28(3): p. 207-214.https://doi.org/10.1007/BF01437887

[20] Aouchiche, H. and F. Medegga, Differential and Integral Cross Sections of Electron Elastic Scattering by PH3 Molecule in the Energy Ranging from 10 eV up to 20 keV. Russian Journal of Physical Chemistry A, 2019. 93(1): p. 116-124.https://doi.org/10.1134/S0036024419010035

[21] Kaur, G., et al., Studies of cross sections for collisions of electrons from hydride molecules: N H 3 and P H 3. Physical Review A, 2015. 91(2): p. 022702.DOI:https://doi.org/10.1103/PhysRevA.91.022702

[22] Itikawa, Y., Cross sections for electron collisions with ammonia. Journal of Physical and Chemical Reference Data, 2017. 46(4): p. 043103.https://doi.org/10.1063/1.5001918

[23] Szmytkowski, C., et al., Total absolute cross section measurements for electron scattering on NH3, OCS and N2O. Journal of Physics B: Atomic, Molecular and Optical Physics, 1989. 22(3): p. 525.https://doi.org/10.1088/0953-4075/22/3/015

[24] Szmytkowski, C., et al., Scattering of electrons from hydride molecules:

PH3. Journal of Physics B: Atomic, Molecular and Optical Physics, 2004. 37(9): p. 1833.https://doi.org/10.1088/0953-4075/37/9/005

[25] Zecca, A., G.P. Karwasz, and R.S. Brusa, Total-cross-section measurements for electron scattering by NH 3, SiH 4, and H 2 S in the intermediate-energy range. Physical Review A, 1992. 45(5): p. 2777.https://doi.org/10.1103/PhysRevA.45.2777

[26] Joachain, C., Recent Progress in Theoretical Methods for Atomic Collisions. Atomic and Molecular Physics of Controlled Thermonuclear Fusion, 1983: p. 139-176.https://doi.org/10.1007/978-1-4613-3763-8_4

[27] Bransden, B.H. and C.J. Joachain, Physics of atoms and molecules. 2003: Pearson Education India.

[28] Khalaf, A.A., L-Shell Radiative and Dielectronic Recombination Rate For Some Iron Ions. Journal of University of Babylon, 2017. 25(2).https://www.iasj.net/iasj/download/fadad98f35164986

[29] Tennyson, J., Electron–molecule collision calculations using the R-matrix method. Physics Reports, 2010. 491(2-3): p. 29-76.https://doi.org/10.1016/j.physrep.2010.02.001

[30] Khalaf, A. and F. Ali, ELASTIC SCATTERING OF POSITRONS BY RARE GASES ATOMS AT LOW AND INTERMEDIATE ENERGIES BY USING MULTIPOLE POLARISABILITY POTENTIAL. Journal of Basrah Researches (Sciences), 2007. 33(1A).https://www.iasj.net/iasj/download/7dd3caecf61b2c38

[31] Huber, A., Variational principles in quantum statistical mechanics, in Mathematical Methods in Solid State and Superfluid Theory. 1968, Springer. p. 364-392.https://doi.org/10.1007/978-1-4899-6435-9_14

[32] Jablonski, A., F. Salvat, and C.J. Powell, Evaluation of elastic-scattering cross sections for electrons and positrons over a wide energy range. Surface and Interface Analysis: An International Journal devoted to the development and application of techniques for the analysis of surfaces, interfaces and thin films, 2005. 37(12): p. 1115-1123.https://doi.org/10.1002/sia.2123

[33] Dirac, P.A.M., The principles of quantum mechanics. 1981: Oxford university press.

[34] Salvat, F., J. Fernández-Varea, and W. Williamson Jr, Accurate numerical solution of the radial Schrödinger and Dirac wave equations. Computer physics communications, 1995. 90(1): p. 151-168.https://doi.org/10.1016/0010-4655(95)00039-I

[35] Desclaux, J.P., A multiconfiguration relativistic Dirac-Fock program. Computer Physics Communications, 1975. 9(1): p. 31-45.https://doi.org/10.1016/0010-4655(75)90054-5

[36] Khandker, M.H., et al., Scattering of e±from the neon isonuclear series over the energy range 1 eV–0.5 GeV. Japanese Journal of Applied Physics, 2020. 59(SH): p.

SHHA05.https://doi.org/10.35848/1347-4065/ab7474

[37] Furness, J. and I. McCarthy, Semiphenomenological optical model for electron scattering on atoms. Journal of Physics B: Atomic and Molecular Physics (1968-1987), 1973. 6(11): p. 2280.https://doi.org/10.1088/0022-3700/6/11/021

[38] O'Connell, J. and N. Lane, Nonadjustable exchange-correlation model for electron scattering from closed-shell atoms and molecules. Physical Review A, 1983. 27(4): p. 1893.https://doi.org/10.1103/PhysRevA.27.1893

[39] Hahn, B., D. Ravenhall, and R. Hofstadter, High-energy electron scattering and the charge distributions of selected nuclei. Physical Review, 1956. 101(3): p. 1131.https://doi.org/10.1103/PhysRev.101.1131

[40] Salvat, F., Optical-model potential for electron and positron elastic scattering by atoms. Physical Review A, 2003. 68(1): p. 012708.https://doi.org/10.1103/PhysRevA.68.012708

[41] Hassan, R., et al., Scattering of e $$^\pm $$±off silver atom over the energy range 1 eV–1 MeV. The European Physical Journal D, 2021. 75(7): p. 1-23.https://doi.org/10.1140/epjd/s10053-021-00222-4

[42] Billah, M.M., et al., Theoretical investigations of e±–CO scattering. Journal of Physics B: Atomic, Molecular and Optical Physics, 2021. 54(9): p. 095203.https://doi.org/10.1088/1361-6455/abf6b4

[43] Ismail Hossain, M., et al., Elastic scattering of electrons and positrons by atomic magnesium. The European Physical Journal D, 2016. 70(2): p. 1-9.https://doi.org/10.1140/epjd/e2016-60527-9

[44] Haque, A., et al., A study of the critical minima and spin polarization in the elastic electron scattering by the lead atom. Journal of Physics Communications, 2018. 2(12): p. 125013.https://doi.org/10.1088/2399-6528/aaf6bd

[45] Khalf, A., Molecules Ionization by Elementary Particles at Incident Energies from threshold to 1KeV. J. Qadisiya, 2007. 12: p. 195.https://www.iasj.net/iasj/download/f4cd6f1f95e39ffb

[46] Blanco, F., L. Ellis-Gibbings, and G. García, Screening corrections for the interference contributions to the electron and positron scattering cross sections from polyatomic molecules. Chemical Physics Letters, 2016. 645: p. 71-75.https://doi.org/10.1016/j.cplett.2015.11.056

[47] Haque, M., et al., e±Ar scattering in the energy range 1 eV≤ Ei≤ 0.5 GeV. Journal of Physics Communications, 2019. 3(4): p. 045011.https://doi.org/10.1088/2399-6528/ab16a0

[48] Gianturco, F., Ab initio model calculations to treat electron scattering from polar polyatomic targets: H2S and NH3. Journal of Physics B: Atomic, Molecular and Optical Physics, 1991. 24(21): p.

4627.https://doi.org/10.1088/0953-4075/24/21/014

[49] D. T. Alle, R.J.G., S. J. Buckman, and M. J. and Brunger, J. Phys. B, 1979.https://iopscience.iop.org/article/10.1088/0953-4075/27/12/018/meta

[50] Shyn, T. and S. Cho, Vibrationally elastic scattering cross section of water vapor by electron impact. Physical Review A, 1987. 36(11): p. 5138.https://doi.org/10.1103/PhysRevA.36.5138

[51] Munjal, H. and K. Baluja, Low-energy electron scattering with polar molecule NH 3 using the R-matrix method. Physical Review A, 2006. 74(3): p. 032712.https://doi.org/10.1103/PhysRevA.74.032712

[52] Rescigno, T., et al., Ab initio description of polarization in low-energy electron collisions with polar molecules: Application to electron-NH 3 scattering. Physical Review A, 1992. 45(11): p. 7800.https://doi.org/10.1103/PhysRevA.45.7800

[53] Sali, N. and H. Aouchiche, Differential and integral cross sections for electron elastic scattering by ammonia for incident energies ranging from 10 eV to 20 KeV. Revista mexicana de física, 2018. 64(5): p. 498-506.

[54] Jain, A.K., A. Tripathi, and A. Jain, Elastic electron collision cross sections for ammonia molecules in the energy range 0.1–1.0 keV. Physical Review A, 1989. 39(3): p. 1537https://doi.org/10.1103/PhysRevA.39.1537.

[55] Harshbarger, W.R., A. Skerbele, and E.N. Lassettre, Generalized oscillator strength of the Ã← X̃ transition of ammonia. The Journal of Chemical Physics, 1971. 54(9): p. 3784-3789.https://doi.org/10.1103/PhysRevA.39.1537

[56] Jain, A., Theoretical study of the total (elastic+ inelastic) cross sections for electron-H2O (NH3) scattering at 10-3000 eV. Journal of Physics B: Atomic, Molecular and Optical Physics, 1988. 21(5): p. 905.https://doi.org/10.1088/0953-4075/21/5/018

[57] Sueoka, O., S. Mori, and Y. Katayama, Total cross sections for positron and electron collisions with NH3 and H2O molecules. Journal of Physics B: Atomic and Molecular Physics (1968-1987), 1987. 20(13): p. 3237.https://doi.org/10.1088/0022-3700/20/13/028.